

# Validation of a MELCOR model of Reactor Cavity Cooling System through support of CFD simulation

Maciej Szudarek<sup>1</sup>, Maciej Skrzypek<sup>2</sup>, Piotr Prusiński<sup>2</sup>, Eleonora Skrzypek<sup>2</sup>

<sup>1</sup> *Warsaw University of Technology, Institute of Metrology and Biomedical Engineering  
Św. Andrzeja Boboli 8, 02-525 Warsaw, Poland*

<sup>2</sup> *National Centre for Nuclear Research, A. Sołtana 7, 05-400 Otwock, Poland*

*Email(s): [maciej.szudarek@pw.edu.pl](mailto:maciej.szudarek@pw.edu.pl), [maciej.skrzypek@ncbj.gov.pl](mailto:maciej.skrzypek@ncbj.gov.pl), [piotr.prusinski@ncbj.gov.pl](mailto:piotr.prusinski@ncbj.gov.pl), [eleonora.skrzypek@ncbj.gov.pl](mailto:eleonora.skrzypek@ncbj.gov.pl)*

**Abstract** – *This work aimed to validate a MELCOR model of the Reactor Cavity Cooling System (RCCS) by conducting Computational Fluid Dynamics (CFD) simulations. The development of a passive heat removal system design falls under the category of safety systems, which require guaranteed functionality and verification during the licensing process for the construction and operation of nuclear reactors, both under normal operating conditions and during accident scenarios. In the High-Temperature Gas-cooled Reactor (HTGR), the containment structure differs from typical Light Water Reactors (LWRs) and is typically designed to be non-leak-tight confinement. Therefore, the RCCS plays a crucial role as a safety function, aiming at residual heat removal to maintain fuel temperature below a limit (set at 1600°C) during an accident scenario with increased fission product release probability. The purpose of this work was to develop a methodology for modelling such systems and to identify the key flow phenomena and challenges to be faced. CFD model sensitivity analysis was performed, and discrepancies between MELCOR and CFD were explained. The observed output quantities were temperatures of system components and heat flux distribution between radiation and convection. Differences in solid bodies temperatures between MELCOR and CFD were in the range of 10 K. Mesh density and turbulence model had negligible influence on temperatures.*

**Keywords:** HTGR, RCCS, research reactor

## I. Introduction

As a result of the establishment of the Polish energy policy framework, which included the High-Temperature Gas-cooled Reactor (HTGR) technology in the Strategy for Responsible Development [1], the national GOSPOSTRATEG-HTR project was carried out, aiming at a pre-conceptual design development for a research HTGR TeResa. In the paper [2], the series of investigations with the use of thermal-hydraulic, neutronic, Monte Carlo Burnup (MCB), and Computational Fluid Dynamics (CFD) codes are described.

The current work focuses on the passive heat removal performance of the Reactor Vessel Cavity Cooling System (RCCS) of TeResa. The development of a passive heat removal system design falls under the category of safety systems, which require guaranteed functionality and verification during the licensing

process for the construction and operation of nuclear reactors, both under normal operating conditions and during accident scenarios.

In the High-Temperature Gas-cooled Reactor (HTGR), the containment structure differs from typical Light Water Reactors (LWRs) and is typically designed to be non-leak-tight confinement. Therefore, the RCCS plays a crucial role as a system performing the safety function of radioactivity confinement by residual heat removal and maintaining the fuel temperature below a limit (set at 1600°C) during an accident scenario with increased fission product release probability. The RCCS removes decay heat by passive cooling via radiation, natural convection and conduction.

Although, having in mind the general rule that there are requirements and guides needed to be applied to each reactor type [3, 4], the specific technical solutions differ from each other, even for the HTGRs

— “each facility’s RCCS design is unique”, as noted in [5]. No standards make appropriate heat transfer analysis on a system level a non-trivial task. In this context, partial validation of the applied correlations and modelling assumptions with CFD tools is a widely used approach.

An overview of passive heat removal systems is presented in [6]. In [7], an air-cooled helical RCCS immersed in a water pool was studied. This unusual design was meant to address weak points of typical air-cooled (weak cooling ability) and water-cooled (complex structure) RCCS systems. Based on an experimental study aided with CFD, heat transfer coefficients for system models were developed. [8] presents a CFD study on RCCS for Very High-Temperature Gas-Cooled Reactors (VHTRs), where the design is similar to the one in the present paper. Various cases were investigated numerically, with different geometries and boundary conditions. [9] describe a thermo-hydraulic model of VHTR’s RCCS, which includes a fuel block. Static and transient cases are validated against experimental results from [10].

The purpose of this work is to develop a methodology for modelling RCCS and to identify the key flow phenomena and challenges to be faced. It was necessary to validate the system model prepared in MELCOR [11], which involved unavoidable simplifying assumptions. CFD model sensitivity tests were performed, and discrepancies between MELCOR and CFD were explained. The observed output quantities were temperatures of system components and heat fluxes due to radiation and convection. The obtained results were compared with observations from other research papers.

## II. Materials and methods

### II.A. MELCOR model

The MELCOR code is a widely recognized tool for the analysis of the accident progression for various reactor types. It was demonstrated to be a suitable tool for severe accident progression, source term and consequence analysis evaluations for non-LWR reactors in [12] and [13].

The MELCOR model used for the investigation was based on the reactor design data described in [2]. The model was developed based on the methodology presented in [14]. The applied discretization of the Reactor Pressure Vessel (RPV), core with active and inactive components, RPV cavity and the RCCS is shown in Fig. 1. The core is made of 6 rings, and it was divided into 12 nodes vertically. Above and below the active core region, there are upper and lower reflectors with 3 and 4 nodes, respectively. Each node

corresponds to a height of 0.4 m. The thermal energy generated in the core is removed by a helium coolant.

Additionally, heat from the core is radiated through the outside of the RPV to RCCS, which is designed to consist of 260 equidistant vertical pipes connected with flat fins distributed around the perimeter. Every other pipe belongs to one of the two RCCS subsystems for redundancy, and water flowing through the circular tubes removes the heat from the system to the water tank connected to the cooling tower. From the radiation calculations point of view, the RCCS surface is treated as a cylinder.

The model of the MELCOR RCCS is nodalized using the “slice technique”, with the cell levels corresponding to the RPV and cavity heights. The assumptions made for the heat transfer between the cavity volume and the RCCS is based on the free convection between two heat structure components (HS) and control volume component (CV) [12]. The HS component (MELCOR specific component) is able to transfer heat to and from the CV based on the calculated  $h$  [ $W/m^2K$ ], derived upon the internal CVs flow regime. The heat transfer coefficient, in MELCOR 2.2.11, code is calculated on the following basis:

$$h = \max(Nu_{laminar}, Nu_{turbulent}), \quad (1)$$

where for the HTGR (the gas cooled surfaces in the calculation domain) the laminar and turbulent free convection coefficients are calculated following the relation [15]:

$$Nu = 0.046 \cdot Ra^{1/3}. \quad (2)$$

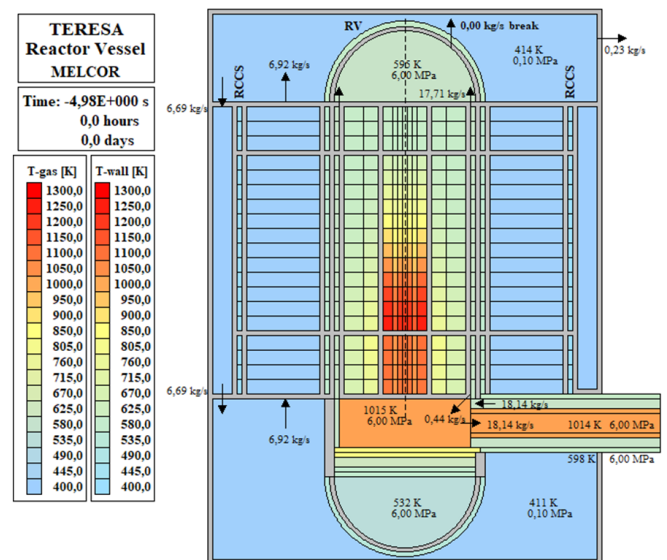


Fig. 1. MELCOR model of the TeResa reactor vessel.

Reynolds number is calculated based on hydraulic diameter, mean velocity and local fluid parameters. Prandtl number is calculated from the local fluid properties.

The air inner cavity between the reactor pressure vessel (RPV) and the RCCS has a single node in the radial direction to remove the possibility of artificial flow patterns. It also reduces model complexity and related uncertainties. Forced convection of air in the inner cavity was assumed with a mass flow rate of 6.92 kg/s.

The RCCS is separated from the outer wall of the confinement by the outer air cavity.

## II.B. CFD model

The CFD model was prepared in commercial software ANSYS Fluent 2023 R1. For this preliminary study, an axisymmetric section consisting of RPV, inner air cavity, RCCS and outer air cavity was prepared. RPV had 7.8 m of total height and 4.8 m of active core height. RCCS height was also equal to 7.8 m. All relevant model dimensions are shown in Fig. 2.

A heat flux profile from MELCOR was applied as the boundary condition on the inner RPV wall. The inner and outer air cavities are connected in a single cavity in the baseline case. The flow of water in RCCS was not modelled; a convective boundary condition was used with a heat transfer coefficient derived from the Dittus-Boelter correlation. All of the other walls were considered adiabatic. It was verified that the shape of the upper and lower parts of the cavity does not influence the results significantly.

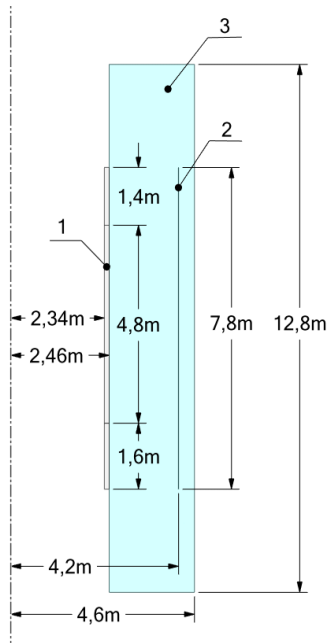


Fig. 2. CFD model computational domain; 1— RPV, 2 — RCCS, 3 — air cavity.

A quad-dominant mesh was used. To resolve thermal and velocity boundary layers, 30 prismatic elements were generated with a growth rate of 1.1 and dimensionless wall distance  $y^+$  below 1. The baseline grid characteristic element size was 4 cm. An overview of the generated mesh is shown in Fig. 3.

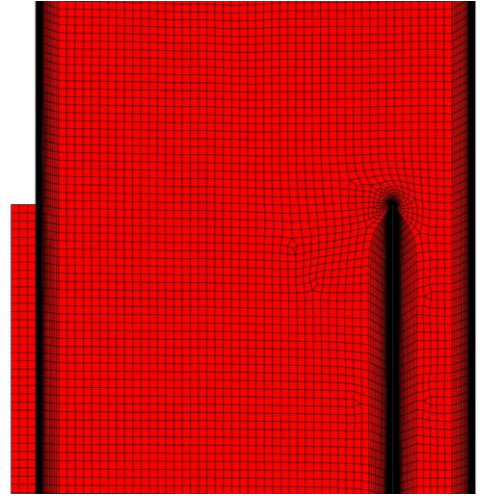


Fig. 3. Baseline grid, zoomed-in view.

The modelled scenario concerns turbulent flow driven by natural convection. The Rayleigh number  $Ra$  was estimated using the eq. (3):

$$Ra = \frac{c_p \cdot g \cdot \rho \cdot \beta \cdot \Delta T \cdot H^3}{\mu \cdot k} \approx 4 \cdot 10^{11} \quad (3)$$

where  $c_p$  is the specific heat of air,  $g$  is gravitational acceleration,  $\rho$  is the air density,  $\beta$  is thermal expansion coefficient,  $\Delta T$  is the temperature difference which is the driving force for natural convection,  $H$  is the RCCS height,  $\mu$  is air dynamic viscosity, and  $k$  is air thermal conductivity.

Because of the low- $Re$  approach,  $k-\omega$  SST turbulence model was used in the baseline case. Material properties of air and steel matched between MELCOR and CFD. They were introduced as a function of temperature, and an incompressible-ideal gas model was used to describe air density. No radiation absorption was considered, so a surface-to-surface (S2S) radiation model without clustering was used to calculate radiative heat fluxes.

Calculations were performed with a coupled pseudo-transient pressure-velocity scheme with a pseudo time step size of 1 s, using the least-square cell-based scheme for gradients, body force weighted scheme for pressure, and second-order upwind discretization schemes for all the other equations. Velocity oscillations were present in the lower and upper regions of the domain, where the inner and outer

cavities merged. Therefore for each case, 4000 iterations were run, and the results were sampled over the last 2000 iterations of captured steady oscillations.

### III. Results and Discussion

In the study, a steady-state case with a nominal core power was considered, where power distribution along the height of the core corresponded with axial Middle of Cycle distribution (MOC), and radial power distribution was assumed as flat. It gives relatively uniform heat flux distribution on the RPV wall, as shown in Fig. 4.

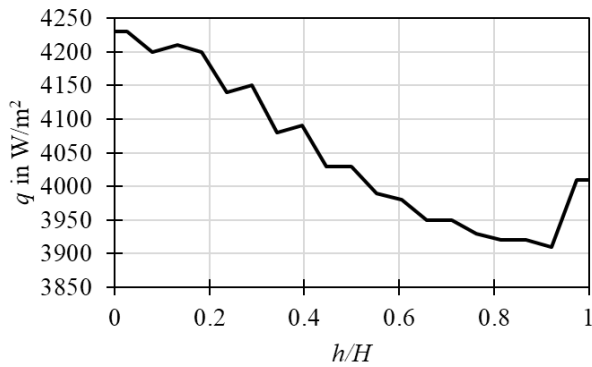


Fig. 4. Axial heat flux at the inner RPV wall.

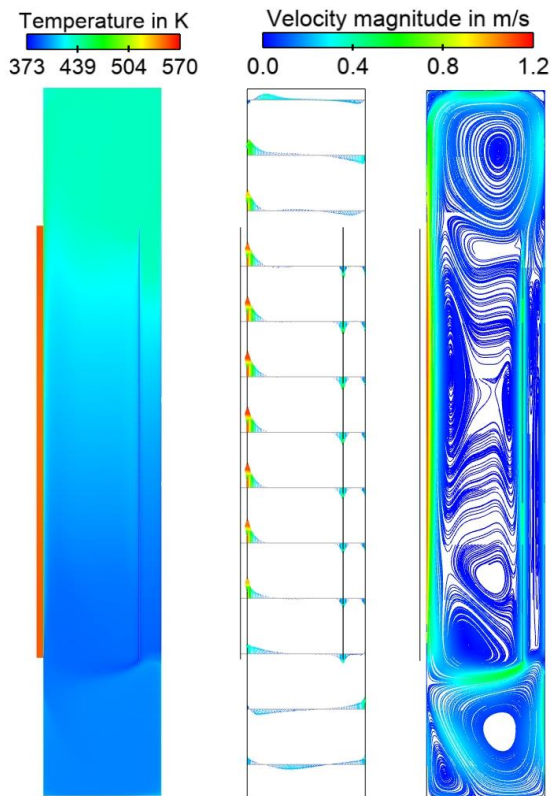


Fig. 5. Temperature contours, velocity vectors and pathlines coloured by velocity magnitude in the baseline case.

Temperature and velocity fields from CFD calculations are shown in Fig 5. RPV temperature reaches 570 K, and a steep temperature gradient is present in the radial direction. Air velocity reaches 1.2 m/s near the middle of the RPV wall height. A single dominating recirculation cell is present, where the heated air from the RPV side is lifted towards the upper wall of the fluid domain and then is split between the inner and outer air cavities, where it is cooled down from both sides of the RCCS water channels. The ratio of radiation to total heat transfer rates is ca. 80%, which is in agreement with other studies [16, 17].

The following figures compare the results between MELCOR and CFD models. As shown in Fig. 6, the temperature on the outer side of the RPV is lower by roughly 10 K in the CFD model. In both cases, the temperature profile is flat — the temperature difference along the RPV height does not change by more than 10 K.

Three grid sizes with 1 cm, 2 cm and 4 cm characteristic sizes were compared to check for mesh independence of the results. The temperatures of the RPV wall are not strongly affected by the grid density—the difference in maximal temperatures of the RPV is lower than 1%. Various turbulence models were tested, and the differences in local RPV temperatures between  $k-\omega$  SST, realizable  $k-\epsilon$  with enhanced wall treatment and Spalart-Allmaras turbulence models do not exceed 3 K.

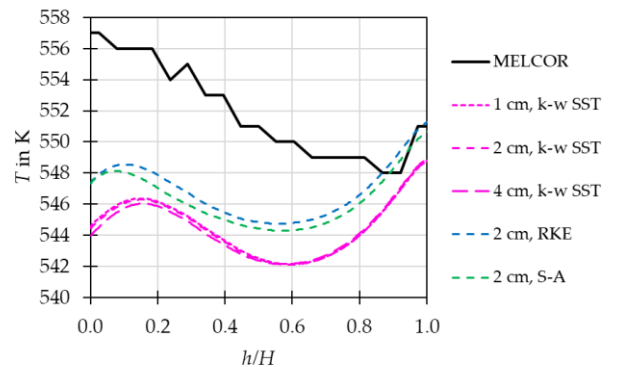


Fig. 6. Temperature profiles along the height of the outer RPV surface.

By analyzing the total surface heat fluxes at the outer RPV surface, shown in Fig. 7, one can observe a peak at the lower edge of the RPV in CFD in the range of 0-0.05  $h/H$ , corresponding to the developing thermal boundary layer. This effect has an insignificant contribution to the total heat transfer rate due to its relatively small area.



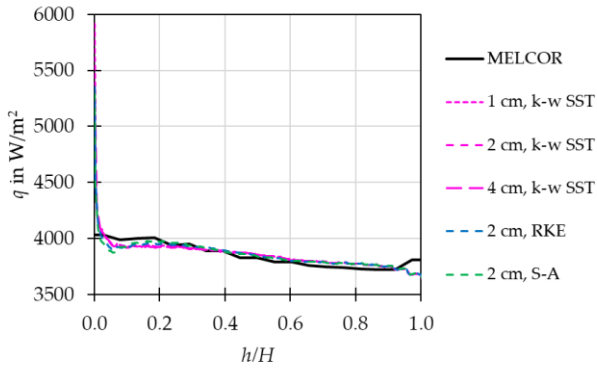


Fig. 7. Total surface heat flux along the height of the outer RPV surface.

The local radiation heat fluxes are lower in the CFD case by ca. 15%, as shown in Fig. 8.

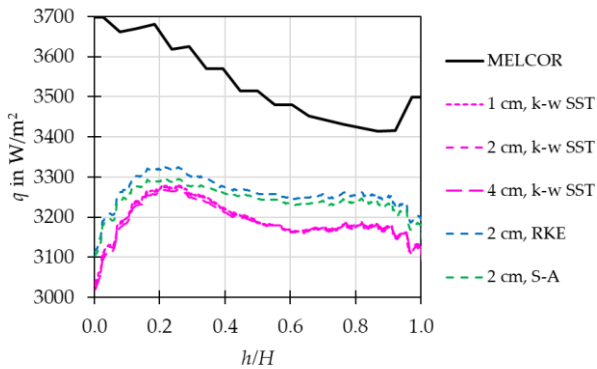


Fig. 8. Radiation surface heat flux along the height of the outer RPV surface.

The temperature and velocity of the air in the inner cavity are compared in Figs. 9 and 10, respectively. CFD results were averaged spatially to mimic MELCOR discretization.

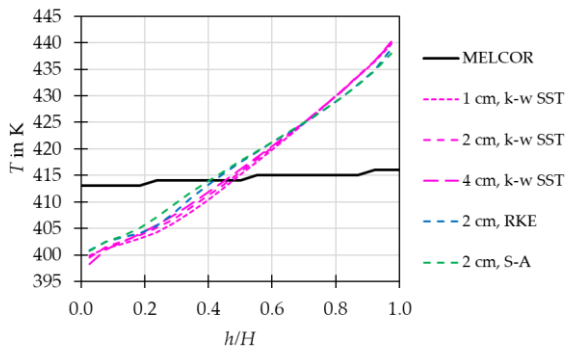


Fig. 9. Air temperature distribution in the inner cavity, averaged radially.

In the MELCOR case, the high mass flow in the cavity volume is present, and the air temperature is uniform in the vertical direction. In CFD, natural convection is modelled, and thermal stratification is observed. Also, the grid size has a significant impact

on the average air velocity in the inner cavity. However, because the radiation dominates in the total heat transfer rate and the air velocity values are small, this sensitivity to the mesh size does not translate to significant temperature differences.

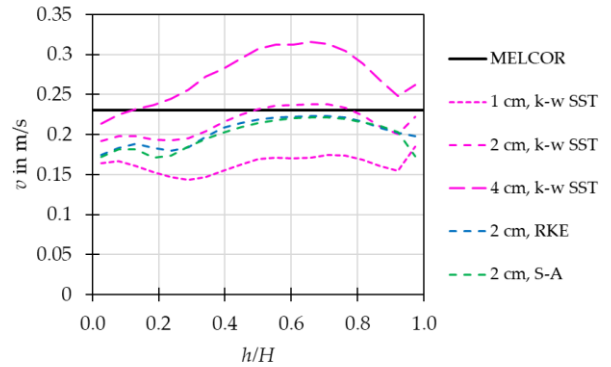


Fig. 10. Air velocity magnitude distribution in the inner cavity, averaged radially.

An additional set of CFD analyses was performed to address the significance of a conditions present in the cavity volume in the MELCOR model, where significant flow was established.

In case #2, the outer cavity is not modelled, and the domain is limited to the RCCS height in the vertical direction. The flow is forced with the same mass flow rate of 6.92 kg/s and temperature of 411 K as in the MELCOR model. Natural convection is still included.

In case #3, the outer cavity is excluded from the domain, and there is no forced convection. Top and bottom cavity surfaces are treated as walls.

Case #4 transforms case #3 to the three-dimensional slice of the geometry, which extends circumferentially to a single pair of RCCS tubes with a symmetry boundary condition on side surfaces. All the geometries are shown in Fig. 11.

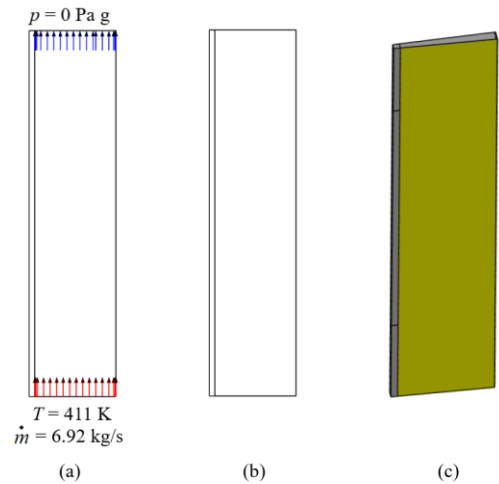


Fig. 11. CFD domains used in additional tests: (a) Case #2; (b) Case #3; (c) Case #4.

Temperatures at the outer RPV wall for cases 1-4 are compared in Fig. 12. Cases #2 and #3 promote more intensive convective heat transfer, hence lower temperatures. Values for 3D case #4 were averaged circumferentially, and they match well with the two-dimensional axisymmetric case #3.

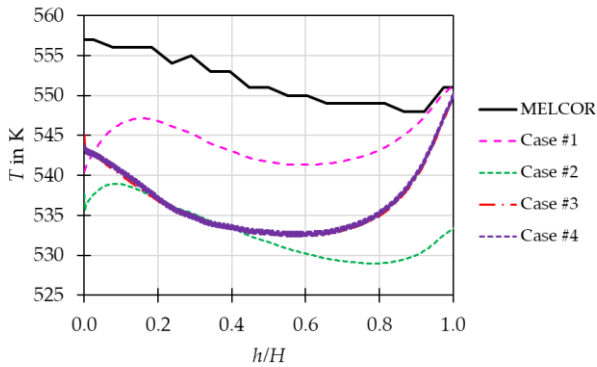


Fig. 12. Comparison of temperatures at the outer RPV wall for cases 1-4.

Temperatures and velocities for cases 1-4 are compared in Figs. 13 and 14, respectively. Values for 3D case #4 were captured in the mid-plane between tubes. In case #2, the stream injected through the inlet attaches to the hot RPV wall. In cases #3 and #4, a single recirculation cell forms.

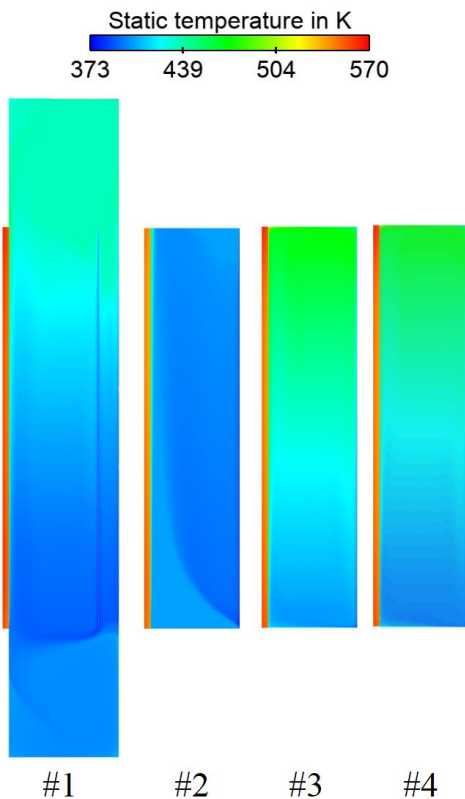


Fig. 13. Comparison of temperature fields for cases 1-4.

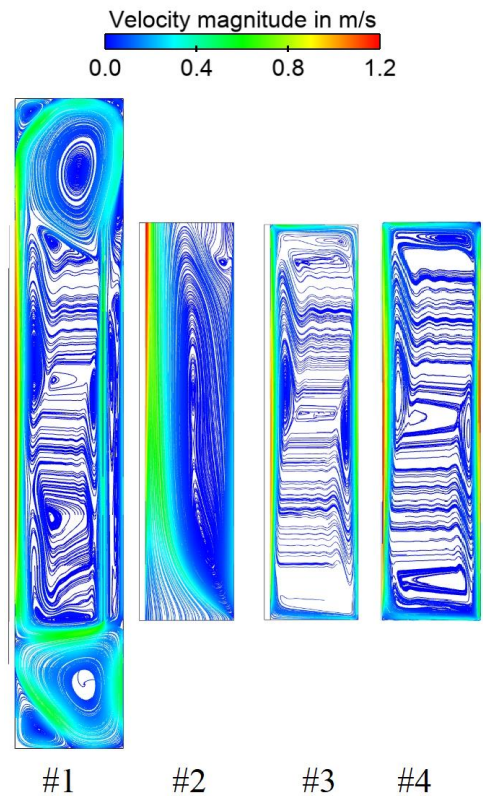


Fig. 14. Comparison of velocity fields for cases 1-4.

None of the analysed models includes the heating of the flat fins between water tubes, which then radiate heat towards the outer cavity. The effect will vary depending, e.g. on the number of water tubes, but according to the study [8], this can contribute up to 13% of the total heat transfer rate.

#### IV. Conclusions

A comparison of preliminary MELCOR and CFD models of RCCS was presented. CFD model sensitivity tests were performed, and discrepancies between MELCOR and CFD were explained.

The MELCOR model overestimated temperatures in all the studied configurations. The difference in RPV temperatures between MELCOR and CFD was in the range of 10 K. Mesh density and turbulence model had negligible influence on the observed results.

Some difference in the established flow in the cavity between CFD and MELCOR results have been found. This has influence on the thermal stratification, which is not visible in the MELCOR results and has the largest impact on temperature distribution in the inner part of the cavity. This may become important in other reactor design points.

Judging from the comparison of cases #1, #3 and #4, domain height or three-dimensional flow features

do not have a significant impact on the result in this particular case.

Both in MELCOR and 2D axisymmetric simulations the RCCS surface was treated as a cylinder. This simplification affects the computed view factors and may lead to underestimated RPV temperatures. A preliminary 3D simulation was made to assess the impact of this simplification on the obtained temperatures. Although the differences in temperatures were negligible, this might not be the case in general.

Further work will focus on 3-dimensional CFD models, including RCCS tubes, and comparing various design points to develop more general conclusions, which can then be implemented in the integral code. Other topics which will be investigated are exploratory computation on the system efficiency with various water mass flow rates, system redundancy tests, and possibilities of minimizing cost by reducing the overall dimensions and mass of the enclosure.

## Acknowledgements

This work is part of the studies in the strategic Polish program of scientific research and development work “Social and economic development of Poland in the conditions of globalizing markets GOSPOSTRATEG”, part of “Preparation of legal, organizational and technical instruments for the HTR implementation” co-financed by the National Centre for Research and Development (NCBiR) in Poland.

## References

1. Appendix to Resolution No. 8 of the Council of Ministers of 14 February 2017 on the Adoption of the Strategy for Responsible Development for the Period up to 2020 (Including the Perspective up to 2030). Available online: <http://isap.sejm.gov.pl/isap.nsf/DocDetails.xsp?id=WMP20170000260> (accessed on 8 February 2022).
2. Skrzypek, E., Muszyński, D., Skrzypek, M., Darnowski, P., Malesa, J., Boettcher, A., & Dąbrowski, M. P. (2022). Pre-Conceptual Design of the Research High-Temperature Gas-Cooled Reactor TeResa for Non-Electrical Applications. *Energies*, 15(6). <https://doi.org/10.3390/en15062084>
3. IAEA Specific Safety Requirements No. SSR-2/1 (Rev. 1)
4. Specific Safety Requirements for Design of Modular High-Temperature Gas-Cooled Reactors (IAEA CRP I31026)
5. Capone, L., Hassan, Y. A., & Vaghetto, R. (2011). Reactor cavity cooling system (Rccs) experimental characterization. *Nuclear Engineering and Design*, 241(12), 4775-4782.
6. Lisowski, D., Lv, Q., Alexandreanu, B., Chen, Y., Hu, R., & Sofu, T. (2021). An Overview of Non-LWR Vessel Cooling Systems for Passive Decay Heat Removal (Technical Letter Final Report).
7. Oh, C. H., Park, G. C., & Davis, C. (2009). RCCS experiments and validation for high-temperature gas-cooled reactor. *Nuclear Technology*, 167(1), 107–117. <https://doi.org/10.13182/NT09-A8855>
8. Frisani, A., & Hassan, Y. A. (2014). Computation fluid dynamics analysis of the Reactor Cavity Cooling System for Very High Temperature Gas-Cooled Reactors. *Annals of Nuclear Energy*, 72, 257–267. <https://doi.org/10.1016/j.anucene.2014.04.039>
9. Tsuji, N., Nakano, M., Takada, E., Tokuhara, K., Ohashi, K., Okamoto, F., Tazawa, Y., Inaba, Y., & Tachibana, Y. (2014). Study of the applicability of CFD calculation for HTTR reactor. *Nuclear Engineering and Design*, 271, 564–568. <https://doi.org/10.1016/j.nucengdes.2013.12.033>
10. Nakagawa, S., Fujimoto, N., Shimakawa, S., Nojiri, N., Takada, T., Saikusa, A., ... & Iyoku, T. (2002). Rise-To-Power Test in High Temperature Engineering Test Reactor. Japan Atomic Energy Research Institute (JAERI), JAERI Report, JAERI-Tech, 69.
11. Humphries, L. MELCOR Computer Code Manuals; Version 2.2.11932; Sandia National Laboratories: Albuquerque, NM, USA, 2018; Volumes 1 & 2.
12. NRC Non-Light Water Reactor Near-Term Implementation Action Plans, ML 17165A069, July 2017
13. Wagner, K. C., Beeny, B. A., Luxat, D. L., Gelbard, F., Louie, D. L., Albright, L. I., & Humphries, L. L. (2023). MELCOR integrated severe accident code application to safety assessment of high-temperature gas-cooled reactors. *Nuclear Engineering and Design*, 402, 112083.
14. Skrzypek, M., Skrzypek, E., Stempniewicz, M., & Malesa, J. (2021, October). Study on the DLOFC Accident of the GEMINI+ Conceptual Design of HTGR Reactor with MELCOR and SPECTRA. In *Journal of Physics: Conference Series* (Vol. 2048, No. 1, p. 012043). IOP Publishing.
15. V. H. Ransom et al., RELAP5/MOD1 Code Manual Volume 1: System Models and Numerical Methods, NUREG/CR-1826, EGG-2070, R2, September 1981.
16. Kunitomi, K., Nakagawa, S., & Shinozaki, M. (1996). Passive heat removal by vessel cooling system of HTTR during no forced cooling accidents. *Nuclear engineering and design*, 166(2), 179-190.
17. Ramiro Freile, Mauricio Tano, Paolo Balestra, Sebastian Schunert, Mark Kimber, Improved natural convection heat transfer correlations for reactor cavity cooling systems of high-temperature gas-cooled reactors: From computational fluid dynamics to Pronghorn, *Annals of Nuclear Energy*, Volume 163, 2021, 108547, ISSN 0306-4549, <https://doi.org/10.1016/j.anucene.2021>